



2021

## Polydopamine and silica nanoparticles magnetic dispersive solid phase extraction coupled with liquid chromatography-tandem mass spectrometry to determine phenolic acids and flavonoids in fruit wine

Follow this and additional works at: <https://www.jfda-online.com/journal>

 Part of the [Food Science Commons](#), [Medicinal Chemistry and Pharmaceutics Commons](#), [Pharmacology Commons](#), and the [Toxicology Commons](#)



This work is licensed under a [Creative Commons Attribution-Noncommercial-No Derivative Works 4.0 License](#).

### Recommended Citation

Lee, Hui-Ling; Kang, Chih-Yuan; Kuo, Yen-Jung; and Tseng, Shan-Ni (2021) "Polydopamine and silica nanoparticles magnetic dispersive solid phase extraction coupled with liquid chromatography-tandem mass spectrometry to determine phenolic acids and flavonoids in fruit wine," *Journal of Food and Drug Analysis*: Vol. 29 : Iss. 3 , Article 1.

Available at: <https://doi.org/10.38212/2224-6614.3359>

This Original Article is brought to you for free and open access by Journal of Food and Drug Analysis. It has been accepted for inclusion in Journal of Food and Drug Analysis by an authorized editor of Journal of Food and Drug Analysis.

# Polydopamine and silica nanoparticles magnetic solid phase extraction coupled with liquid chromatography-tandem mass spectrometry to determine phenolic acids and flavonoids in fruit wine

Hui-Ling Lee <sup>a,\*</sup>, Chih-Yuan Kang <sup>a</sup>, Yen-Jung Kuo <sup>a</sup>, Shan-Ni Tseng <sup>b</sup>

<sup>a</sup> Department of Chemistry, Fu Jen Catholic University, Xinzhuang District, New Taipei City 24205, Taiwan

<sup>b</sup> Department of Textiles & Clothing, Fu Jen Catholic University, Xinzhuang District, New Taipei City 24205, Taiwan

## Abstract

Magnetic solid phase extraction (MSPE) have been widely applied in a variety of sample preparation techniques. Herein, Fe<sub>3</sub>O<sub>4</sub>@pDA as the sorbents for MSPE, were developed for the determination of phenolic acids and flavonoids in fruit wine samples in combination with LC-MS/MS. The Fe<sub>3</sub>O<sub>4</sub>@pDA were characterized by Fourier transform infrared spectroscopy (FT-IR), powder X-ray diffraction (PXRD), transmission electron microscopy (TEM), Superconducting Quantum Interference Device Magnetometer (SQUID) and thermogravimetric analysis (TGA) in detail. In the present study, a new, rapid, and efficient MSPE by LC-MS/MS was established for the extraction and sensitive detection of phenolic acids and flavonoids. Under the optimized condition of extraction procedure including the pH value of 4.0, 10 mg of Fe<sub>3</sub>O<sub>4</sub>@pDA, 60 s extraction time, and 600 μL desorption solvent volume, good responses were investigated. Results showed that the limits of detection (S/N = 3) for phenolic acids and flavonoids were in the range of 0.01–0.29 ng/mL. The correlation coefficients of all analytes were more than 0.9985. The method was satisfactorily used for the detection of eleven analytes, and the recoveries of these targets for the two spiked wines (white grape wine and litchi wine) ranged from 80.03 to 116.68% and from 84.00 to 116.1%, respectively.

**Keywords:** Flavonoids, Fe<sub>3</sub>O<sub>4</sub>@pDA, LC-MS/MS, Magnetic solid phase extraction, Phenolic acids

## 1. Introduction

Phenolic acids and flavonoids, a class of important hydroxylated derivatives of benzoic acids and cinnamic acids [1], commonly used antioxidant and might inhibit diseases such as cardiovascular disease, cancer, chronic disease and human immunodeficiency virus (HIV) [2–4]. These phenolic acids and flavonoids have been known as the major participator in the antioxidant capacity of the herbs, fruits, vegetables, nutritional supplements and wines because of their matrix complexity, then are rarely to analyze [5,6].

To date, various pretreatments such as liquid–liquid extraction (LLE) [7,8], solid-phase

extraction (SPE) [9,10], microwave-assisted extraction (MAE) [11], hollow fiber liquid-phase microextraction (HF-LPME) [12,13], dispersive liquid–liquid microextraction (DLLME) [14] and solid-phase microextraction (SPME), the QuEChERS method et al., have been widely used in phenolic acid samples [15,16]. So far, commercial SPE cartridges have demonstrated good extraction efficiency for six phenolic acids [17], while other sorbents only extract 2–4 types of phenolic acids [18,19]. However, magnetic solid phase extraction (MSPE) has attracted researcher attention due to its advantages of simple operation, biocompatibility, superparamagnetic property, low toxicity and instead of processes such as the centrifugation in traditional dispersive SPE [20,21].

Received 18 January 2021; revised 23 March 2021; accepted 12 May 2021.  
Available online 15 September 2021

\* Corresponding author at: Department of Chemistry, Fu Jen Catholic University, No.510 Zhongzheng Rd. Xinzhuang District, New Taipei City 24205 Taiwan. Fax: +886 2 29023209.  
E-mail address: 076308@mail.fju.edu.tw (H. L. Lee).

<https://doi.org/10.38212/2224-6614.3359>

2224-6614/© 2021 Taiwan Food and Drug Administration. This is an open access article under the CC-BY-NC-ND license (<http://creativecommons.org/licenses/by-nc-nd/4.0/>).

Recent developments have focused on the synthesis of dopamine (DA), which contains catechol and amine functional groups, polydopamine (pDA) can be produced by self-polymerization at a weak alkaline pH [22–25]. The pDA exhibits excellent biocompatibility and adsorption properties and has been considered as an environmentally benign functional material for use in a broad range of biotechnology [26,27], electrochemical [28], nanotechnology [29], and membrane [30] applications. Therefore, we groundbreaking developed simple, and green approach due to  $\text{Fe}_3\text{O}_4$ @pDA has two functions in this extraction such as avoiding centrifugation step and containing the positively charged  $\text{Fe}_3\text{O}_4$ - $\text{NH}_2$  able to catch negatively charged phenolic acids by electrostatic interaction [31,32]. However, simplifying the operation would reduce the whole sample preparation time.

The present research mainly focuses on the synthesize rapid, cost effective, and  $\text{Fe}_3\text{O}_4$  nanoparticles with different surface modifications, characterize them by using TEM and FTIR. MSPE parameters determining the extraction efficiency, including magnetic adsorbent, extraction solvent and desorption solvent, adsorbent amount, desorption solvent volume, extraction time, and desorption time, were investigated. Finally, rapid analysis of low levels of phenolic acids and flavonoids in fruit wine samples by MSPE–HPLC–MS/MS method was demonstrated.

## 2. Experimental

### 2.1. Chemical and reagents

HPLC-grade methanol (MeOH) and HPLC-grade acetonitrile (ACN) were purchased from J.T. Baker. Formic acid and Chlorogenic acid (CGA), Ferulic acid (FA), p-Coumaric acid (p-CMA), Caffeic acid (CA), Gallic acid (GA), Catechin (Cate), Epicatechin (Epi), Rutin (Ru), Quercetin (Que), Hesperetin (Hes), Sinapinic acid (SA), and Ammonium acetate (AA) were purchased from Sigma–Aldrich. Caffeic acid- $^{13}\text{C}_3$  (CA- $^{13}\text{C}_3$ ) and trans-Ferulic acid- $\text{d}_3$  (FA- $\text{d}_3$ ) were purchased from TRC. Acetic acid (HOAc) was purchased from Merck.

### 2.2. Sample preparation method and LC-MS/MS analysis

10  $\mu\text{L}$  aliquot of each wine sample supernatant after centrifugation was added 100 mL 1 mM AA pH 4.0, was diluted with 100 mL 50% MeOH (v/v) and 0.1% formic acid. Then 25  $\mu\text{L}$  diluted wine sample was spiked with 25  $\mu\text{L}$  of internal standards (IS) solution (10 ng  $\text{mL}^{-1}$  caffeic acid- $^{13}\text{C}_3$  and 50 ng

$\text{mL}^{-1}$  ferulic acid- $\text{d}_3$ ) and the solution is vortexed and was stored at  $-20^\circ\text{C}$  till the time of analysis. A 20  $\mu\text{L}$  diluted wine sample was separated by Agilent 1200 HPLC system coupled with an Agilent Eclipse plus C18 (100 mm  $\times$  4.6 mm, 3.5  $\mu\text{m}$ ) column at flow rate of 0.35  $\text{mL min}^{-1}$ . The optimized mobile phase gradient entails the succeeding modifications of mobile phase A (100%  $\text{H}_2\text{O}$ , v/v with 0.1% formic acid) and mobile phase B (100% MeOH, v/v with 0.1% formic acid). The gradient initially started at 50% mobile phase A, which was maintained for 2.5 min, and then changed to 10% mobile phase A in 0.1 min. This composition was maintained for 5.5 min and then ramped to 50% mobile phase A in 0.1 min, and held for 5.6 min at 50% mobile phase A. The total run time was 11 min. After which the next sample was injected. The mass spectrometric data were acquired using a triple-quadrupole mass spectrometer, API 3000 (Applied Biosystem, MDS SCIEX, Concord, Ontario, Canada) which coupled with TurboIonSpray source. The electrospray ionization (ESI) interfaces which was operated in negative ion mode with an ion spray voltage of  $-4200$  V. The turbospray settings were as trails: nebulizer gas pressure at 10 psi, curtain gas at 8 psi, collision activated dissociation (CAD) gas pressure at 6 psi, and the source temperature at  $450^\circ\text{C}$ .

### 2.3. Preparation of $\text{Fe}_3\text{O}_4$ , $\text{Fe}_3\text{O}_4$ @pDA, $\text{Fe}_3\text{O}_4$ @ $\text{SiO}_2$ , $\text{Fe}_3\text{O}_4$ @ $\text{SiO}_2$ @C18 and $\text{Fe}_3\text{O}_4$ @ $\text{SiO}_2$ @APTES

The  $\text{Fe}_3\text{O}_4$  were obtained by a solvothermal method according to a previous report [33]. 2.0 g of  $\text{FeCl}_3 \cdot 6\text{H}_2\text{O}$  and 5.4 g of  $\text{NH}_4\text{OAc}$  were dispersed in 60 mL of ethylene glycol, was stirred continuously for 20 min at  $25^\circ\text{C}$  and then transferred into a Teflon-lined stainless-steel autoclave (100 mL capacity). The solution was heated at  $200^\circ\text{C}$  and maintained for 10 h, and then it was cooled to room temperature, washing was repeated three times by ethanol and water, was dried at  $45^\circ\text{C}$  for further use.

The  $\text{Fe}_3\text{O}_4$ @pDA materials were synthesized according to the reported method [33]. The powder of  $\text{Fe}_3\text{O}_4$  (100 mg) was immersed in 50 mL of 10 mM Tris-HCl buffer (pH 8.5) and 100 mg of dopamine hydrochloride, mixed by ultrasonic apparatus for 5 min and then refluxed for 12 h at room temperature. Subsequently, the product was washed three times with ethanol and water, was dried at  $45^\circ\text{C}$  for further use. The  $\text{Fe}_3\text{O}_4$ @ $\text{SiO}_2$ ,  $\text{Fe}_3\text{O}_4$ @ $\text{SiO}_2$ @C18 and  $\text{Fe}_3\text{O}_4$ @ $\text{SiO}_2$ @APTES materials were synthesized according to the reported methods [34,35]. For  $\text{Fe}_3\text{O}_4$ @ $\text{SiO}_2$  modification, freshly prepared magnetite nanoparticles (0.1 g) dispersed in ethanol (100 mL) and deionized

water (14 mL) and sonicated for 45 min, followed by the addition of aqueous ammonia (3.6 mL, 25%). 0.72 mL of tetraethyl orthosilicate (TEOS) was then added slowly to the reaction solution under mechanical stirring 12 h. For Fe<sub>3</sub>O<sub>4</sub>@SiO<sub>2</sub>@C18 modification, 0.1 g Fe<sub>3</sub>O<sub>4</sub>@SiO<sub>2</sub> and 0.4 mL trimethoxyoctadecylsilane were dissolved in 35 mL toluene, then was kept for 8 h at 80 °C. The product was washed with ethanol for three times and dried. For Fe<sub>3</sub>O<sub>4</sub>@SiO<sub>2</sub>@APTES modification, 0.4 g Fe<sub>3</sub>O<sub>4</sub>@SiO<sub>2</sub> and 0.8 mL 3-aminopropyltriethoxysilane (APTES) were dissolved in 10 mL toluene, then was kept for 12 h at 110 °C. The product was washed with ethanol for three times and dried.

#### 2.4. Characterization of polydopamine microcapsules

The evolution of morphology and structure of synthesized pDA microcapsules were determined by transmission electron microscopy (TEM) on a JEM 2000FXII electron microscope (JEOL, Japan). Powder X-ray diffraction (PXRD) patterns were recorded on a diffractometer (BRUKER D2 PHASER 2nd Generation) for Cu K $\alpha$  radiation ( $\lambda = 1.54184 \text{ \AA}$ ) with a scan speed of 2 s in 2 $\theta$  from 5° to 80°. Fourier-transform infrared spectroscopy (FT-IR) was recorded on a Perkin Elmer 100, and magnetic properties was analyzed on a MPMS3 SQUID (Quantum Design, USA). The thermal stability of the pDA microcapsules was measured by thermogravimetric analysis (Perkin Elmer TGA 7). TGA was performed by heating the specimens from 50 to 900 °C at 10 °C/min in air flow (100 mL/min).

#### 2.5. Magnetic solid phase extraction procedure

The powder of 10 mg of Fe<sub>3</sub>O<sub>4</sub>@pDA were added to 200  $\mu$ L of the standard solution or sample solution. The Fe<sub>3</sub>O<sub>4</sub>@pDA was then collected by applying a magnet to the outer wall of the vial and eluted with 600  $\mu$ L of methanol under vortex for 1 min. The supernatant was collected and filtered through a 0.22  $\mu$ m membrane to eliminate particulate matter before HPLC analysis. MSPE parameters were demonstrated (spiked concentration of 10 ng/mL each for phenolic acids and flavonoids, n = 3), with the initial extraction conditions as follows: sample pH, 4.0; adsorbent amount, 10 mg; extraction time, 60 s; desorption solvent, methanol 600  $\mu$ L in the procedure.

#### 2.6. Method validation

The study was to develop a validated method, so we check the parameters as follows the US FDA [36].

Wine samples collected from two types of wine were analyzed by LC-MS/MS for the presence of phenolic acids and flavonoids, used as the blank wine matrix for the matrix effect test.

##### 2.6.1. Stock solution and calibration curve

Stock standard solutions of phenolic acids and flavonoid at a concentration of 1000  $\mu$ g/mL in MeOH was stored in the refrigerator. Nine concentrations of standard solutions were diluted from 0.1 to 50.0 ng/mL with 50% MeOH (v/v) and 0.1% formic acid and blank wine matrix, and were spiked with a fixed amount of 10 ng/mL caffeic acid-C<sub>3</sub> and 50 ng/mL ferulic acid-d<sub>3</sub> as internal standards (IS). The QC sample was prepared daily in 10 ng/mL standard solution containing IS in neat solvent.

##### 2.6.2. Precision and accuracy

Precision and accuracy were indicated at three spike levels (5, 20, and 100 ng/mL) of the standard solutions in the two wine samples (n = 3) and by calculating the CV (coefficient of variation). Intra-day and inter-day variations spiked with 5, 20 and 100 ng/mL in the two wine samples and calculating the accuracy and CV (coefficient of variation) (n = 3) and obtained on different days from the same two wine samples subject, respectively.

##### 2.6.3. Matrix effect

To study the matrix effect, we injected the mixtures of internal standards in neat solvent and in matrix. The matrix effect was defined as a percent ratio of the mean area of peaks from the standard in the matrix and the mean area of peaks from the standard in neat solvent.

Matrix effects were assessed at nine concentrations for each of the phenolic acids and flavonoids by comparing the peak areas of quintuplicate runs at each concentration for analyte standards in a neat solvent and in the two spiked wine samples. The relative matrix effect was established according to the following formula:

$$\text{ME}\% = \frac{A_{(\text{analyte standards (in diluted wine)})}}{A_{(\text{analyte standards (neat solvent)})}} \times 100\%$$

### 3. Results and discussion

#### 3.1. Characterization of magnetic materials

TEM (Fig. S1 (a)–(e)) displayed a significant difference in color between the neat Fe<sub>3</sub>O<sub>4</sub> and the @pDA, @SiO<sub>2</sub>, @SiO<sub>2</sub>@C18 and @SiO<sub>2</sub>@APTES. TEM images demonstrated a spherical structure with a diameter of 309.4  $\pm$  0.9 nm, 322.6  $\pm$  1.6 nm,

314.0 ± 3.7 nm, 350.5 ± 5.0 nm and 328.2 ± 2.6 nm, respectively (Fig. S1), which indicated that these materials were successfully coated with Fe<sub>3</sub>O<sub>4</sub>. To further demonstrate that the magnetic nanoparticles were favorably coated by @pDA, @SiO<sub>2</sub>, @SiO<sub>2</sub>@C18 and @SiO<sub>2</sub>@APTES, the techniques of FT IR, PXRD, TGA and SQUID were utilized. The FT-IR spectra showed a significant difference in Fig. S2. For the Fe<sub>3</sub>O<sub>4</sub>, the strong absorption peak at 580 cm<sup>-1</sup> was characteristic of Fe–O stretching vibration. For pDA, the adsorption peaks at 3420 and 1604 cm<sup>-1</sup> were assigned to the stretching vibration of O–H and C=C of the catechol structures; the adsorption peaks at 3120 and 1288 cm<sup>-1</sup> could be attributed to N–H bond and C–N stretching vibration. PXRD characterization was applied to further investigate the composition of Fe<sub>3</sub>O<sub>4</sub> and the @pDA, @SiO<sub>2</sub>, @SiO<sub>2</sub>@C18, and @SiO<sub>2</sub>@APTES, and the results are illustrated in Fig. S3, Supporting Information. The PXRD result provided evidence confirming the existence of Fe<sub>3</sub>O<sub>4</sub> in the composite. For Thermal Stability Investigation (Perkin Elmer TGA 7), the thermal stability of Fe<sub>3</sub>O<sub>4</sub> was determined in air with a heating rate of 10 °C/min (Fig. S4). The Fe<sub>3</sub>O<sub>4</sub> @pDA showed two weight loss stages in the 50–900 °C range in the TGA thermogram. The first step degradation (5.86% weight loss) was due to physically combined water below 120 °C. The second weight loss of 38.48% was observed from 120 to 500 °C because of pyrolysis of the remaining organic solvents and thermal decomposition. The magnetic properties of Fe<sub>3</sub>O<sub>4</sub> and the @pDA, @SiO<sub>2</sub>, @SiO<sub>2</sub>@C18, and @SiO<sub>2</sub>@APTES were studied using a vibrating sample magnetometer (Fig. S5). After being coated by @pDA, @SiO<sub>2</sub>, @SiO<sub>2</sub>@C18 and @SiO<sub>2</sub>@APTES, the magnetic response of the Fe<sub>3</sub>O<sub>4</sub> was modified, the saturated magnetization values of Fe<sub>3</sub>O<sub>4</sub> and the @pDA, @SiO<sub>2</sub>, @SiO<sub>2</sub>@C18, and @SiO<sub>2</sub>@APTES were 80.97, 58.14, 55.60, 51.94 and 46.94 emu/g, respectively.

### 3.2. Optimization of extraction conditions for MSPE

To achieve the best separation condition such as pH, amount of adsorbent, extraction time, desorption time and desorption solvent, were studied and optimized for phenolic acids and flavonoids for pre-concentration and clean-up.

#### 3.2.1. Comparison of sorbents and amounts of sorbents

Based on Fig. 1, the Fe<sub>3</sub>O<sub>4</sub>@SiO<sub>2</sub>, Fe<sub>3</sub>O<sub>4</sub>@-SiO<sub>2</sub>@C18 surface is negatively charged at pH 4.0, there is electrostatic repulsion between phenolic

acid and flavonoids. Generally, these phenomena reduce the extraction efficiency in this work. Comparison of these sorbents, isoelectric point of the Fe<sub>3</sub>O<sub>4</sub>@pDA was found to be approximately 4.9, results in the positive charge, which is favorable for the negatively charged target analytes to be adsorbed on Fe<sub>3</sub>O<sub>4</sub>@pDA through the electrostatic attraction. Electrostatic interaction may be the main adsorption mechanism between target analytes and Fe<sub>3</sub>O<sub>4</sub>@pDA. In addition, the amino groups can also form the hydrogen bonds with hydroxyl groups and  $\pi$ - $\pi$  interaction between Fe<sub>3</sub>O<sub>4</sub>@pDA and phenolic acid and flavonoids is stronger than other materials with phenolic acid and flavonoids, and thereby can also contribute the high adsorption. Although surface charge of Fe<sub>3</sub>O<sub>4</sub>@SiO<sub>2</sub>@APTES is also positive, lacking of aromatic rings result in low extraction efficiency. From the abovementioned results, Fe<sub>3</sub>O<sub>4</sub>@pDA was selected for the best sorbent.

To optimize the effect of sorbent quantity on its extraction efficiency for phenolic acids and flavonoids, Fe<sub>3</sub>O<sub>4</sub>@pDA amounts of 3–20 mg were investigated. As shown in Fig. 2, the Fe<sub>3</sub>O<sub>4</sub>@pDA had excellent enrichment ability for the analytes. The adsorption rate increased follow by the sorbent doses from 3 to 20 mg, up to 10 mg is no significant increase of adsorption capacity. Therefore, 10 mg of the Fe<sub>3</sub>O<sub>4</sub>@pDA were used in the following studies.

#### 3.2.2. Effect of sample solution pH

The pH can affect analyte extraction by changing either the stability or the chemical structure of the analytes and the surface charge of the Fe<sub>3</sub>O<sub>4</sub>@pDA [37]. Therefore, sample solution pH was from 2.0 to 10.0 were investigated and the results were shown

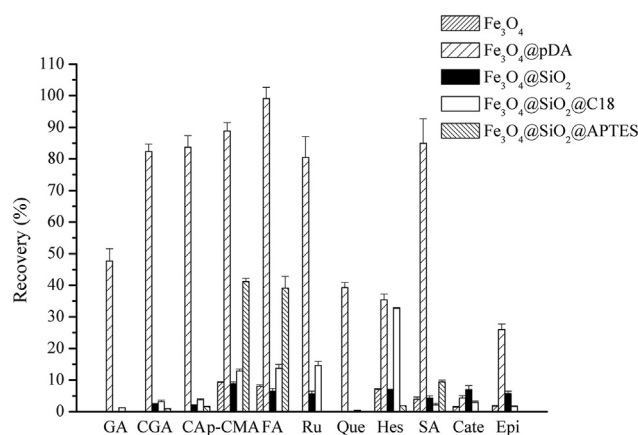


Fig. 1. Comparison of different sorbents on the extraction efficiency of phenolic acids and flavonoids, sorbent amount, 10 mg; pH 4.0; adsorption time, 60 s; desorption solvent, MeOH; desorption solvent volume, 600  $\mu$ L, and desorption time, 60 s.

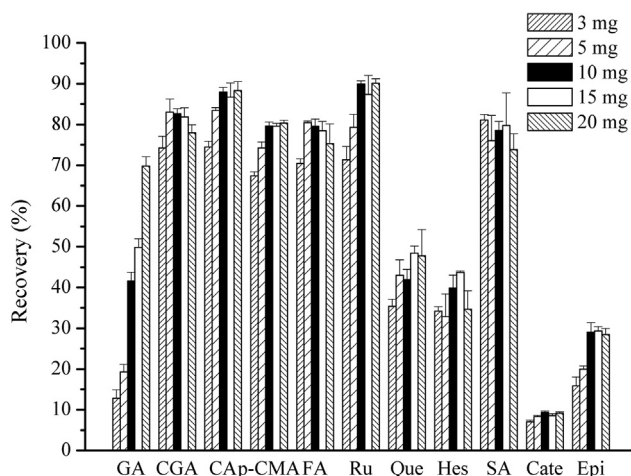


Fig. 2. Influence of the  $\text{Fe}_3\text{O}_4@\text{pDA}$  amount on the extraction efficiency of phenolic acids and flavonoids.

in Fig. 3. The extraction capacity of  $\text{Fe}_3\text{O}_4@\text{pDA}$  increased as the sample pH was increased from 2.0 to 4.0, while decreased as the pH values over 4.0. The phenomenon might be explained that target analytes were almost weak acids with  $\text{pK}_a$  values in the range of 3.14–4.10, so the efficient extraction at pH 4.0 may be attributed to the following factors: electrostatic interaction between negatively charged carboxyl groups of phenolic acids and positively charged  $\text{Fe}_3\text{O}_4@\text{pDA}$ . In addition, the GA ( $\text{pK}_a$  4.0) and Que ( $\text{pK}_a$  7.1) maintained their neutrality and would disturb the electrostatic interaction between Quercetin (Que) and the  $\text{Fe}_3\text{O}_4@\text{pDA}$  adsorbent, resulting in a reduced recovery. Finally, the results show sample solution pH was set at 4.0 for following experiments.

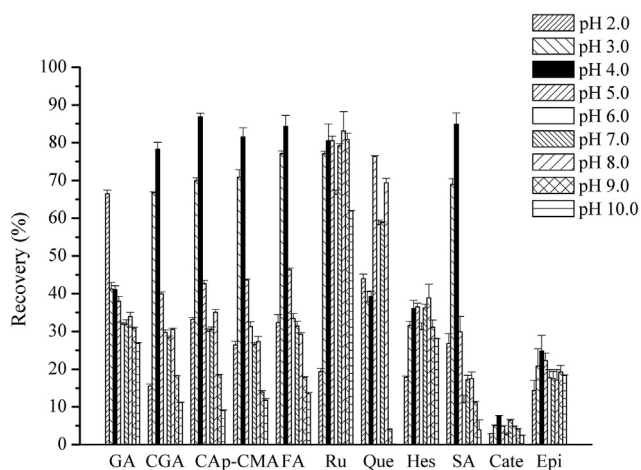


Fig. 3. Effect of sample pH in phenolic acids and flavonoids.

### 3.2.3. Effect of extraction time profile

The extraction time can be an important parameter in adsorption condition. The extraction time was varied from 30 to 600 s, as shown in Fig. 4a, the  $\text{Fe}_3\text{O}_4@\text{pDA}$  showed the adsorption amount decreased slightly before reaching adsorption equilibrium after 180 s. Due to longer extraction times might lead to the dissolution of the analytes into the matrix. For the following analysis, 60 s was selected as the extraction time.

### 3.2.4. Effect of desorption conditions

In the extraction process, the selection of the different polarity solvent for desorption of the target analytes by  $\text{Fe}_3\text{O}_4@\text{pDA}$  is quite essential. According to the principle of like dissolves like, a good choice between the polarities of desorption solvent and target analytes should provide to better recovery. Six organic solvents, including methanol (MeOH), acetone, ACN, ethyl acetate (EA), methyl tert-butyl ether (MTBE) and hexane, were evaluated, Fig. 4b shows that the recovery of phenolic acids and flavonoids reached the maximum when MeOH was used as the desorption solvent. Therefore, MeOH volumes of 200  $\mu\text{L}$ –600  $\mu\text{L}$  were also assessed. As shown in Fig. 4c, desorption solvent of 600  $\mu\text{L}$  achieved the maximum analyte recovery.

To achieve the reliable results, MeOH was studied as the desorption solvent and desorption solvent volume on the extraction efficiency was studied, and also 600  $\mu\text{L}$  was considered the suitable desorption solvent volume for the desorption process. On the other hand, the desorption time of analytes was evaluated in a range of 30–600 s. Fig. 4d shows that after 60 s of desorption, quick equilibrium and no more analyte was detected in the eluent. Finally, the analytes were eluted with 600  $\mu\text{L}$  of MeOH for 60 s in the further analysis.

### 3.3. Reusability of the MSPE

The reusability of the  $\text{Fe}_3\text{O}_4@\text{pDA}$  was evaluated by magnetic properties of the phenolic acids and flavonoids at each adsorption run in first cycle, after 1–4 months of extraction. According to Fig. S6, the magnetic properties remained almost stable, indicating that  $\text{Fe}_3\text{O}_4@\text{pDA}$  was mechanically stable and possessed excellent reusability.

### 3.4. Validation of the optimal extraction condition

The  $\text{Fe}_3\text{O}_4@\text{pDA}$  extraction MSPE was applied to phenolic acids and flavonoids. In the optimal condition,  $\text{Fe}_3\text{O}_4@\text{pDA}$  was validated to determine

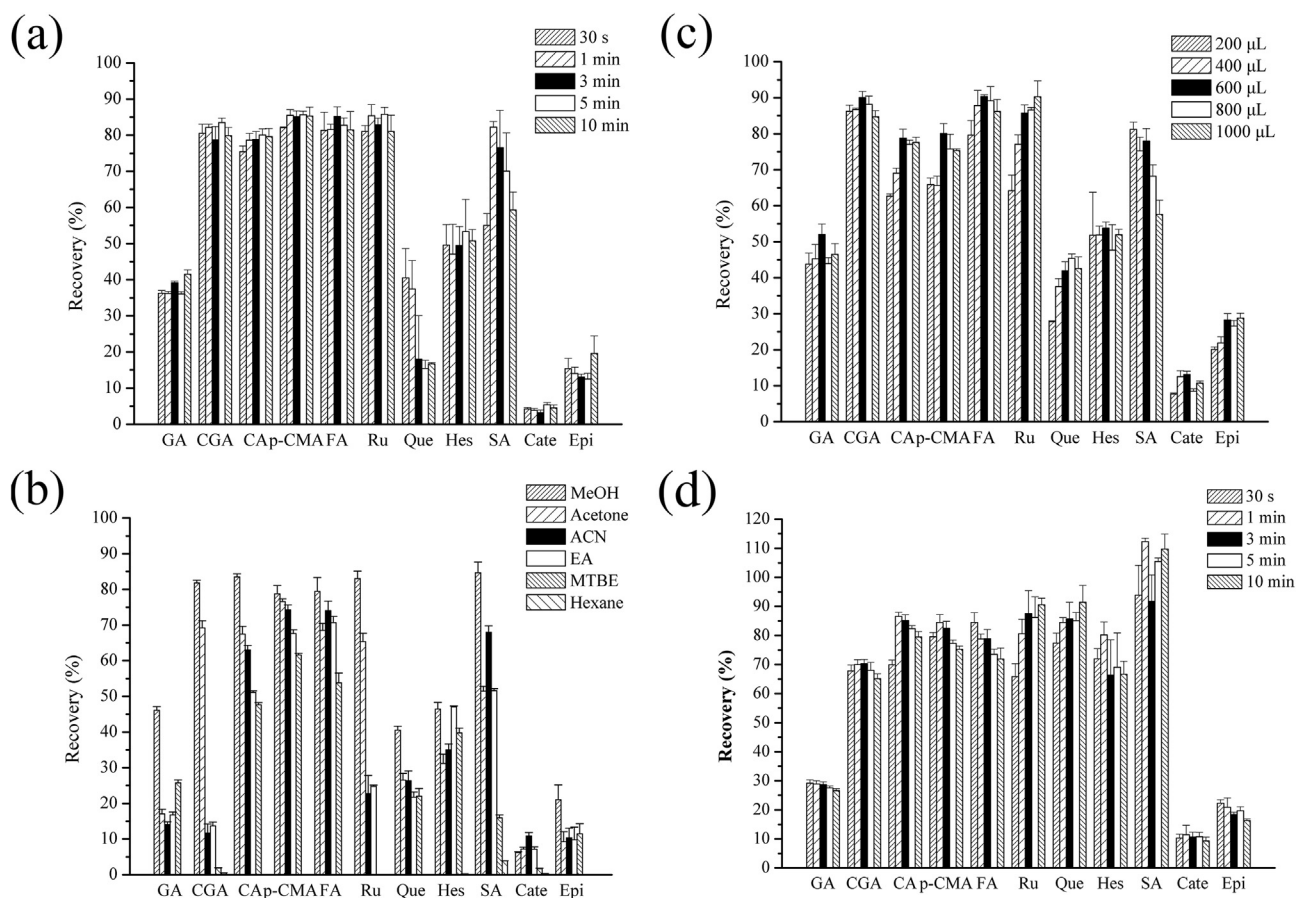


Fig. 4. (a) Liquid–liquid extraction vortex time (b)  $\text{Fe}_3\text{O}_4\text{@pDA}$  of different extraction solvents (c) different extraction solvent volumes and (d) desorption time on the extraction efficiency of phenolic acids and flavonoids.

the accuracy and precision were determined in intra- and inter day and shown in Tables S1 and S2. The obtained extraction recoveries for phenolic acids and flavonoids based on intra and inter day ( $n = 3$ ) were in the range of 84.07–116.68% and 80.33–120.78% in white grape wine and 84.00–116.10% and 83.55–119.42% in litchi wine, respectively. The LOD and LOQ were 0.01–0.29 ng/mL

and 0.02–0.96 ng/mL, respectively (Table 1). The above results demonstrated the good repeatability and reproducibility of the  $\text{Fe}_3\text{O}_4\text{@pDA}$ .

### 3.5. Real sample analysis

In order to evaluate the applicability of the  $\text{Fe}_3\text{O}_4\text{@pDA}$ , it was selected to extract phenolic

Table 1. Linearity and sensitivity of phenolic acid and flavonoids analysis by LC-MS/MS.

| Analyte                 | Calibration range (ng/mL) | Retention time (min) | Calibration curves     | Correlation coefficient ( $R^2$ ) | LOD <sup>a</sup> (ng/mL) | LOQ <sup>b</sup> (ng/mL) |
|-------------------------|---------------------------|----------------------|------------------------|-----------------------------------|--------------------------|--------------------------|
| Gallic acid (GA)        | 0.1–50                    | 3.34                 | $y = 8.4776x + 2.5480$ | 0.9992                            | 0.01                     | 0.02                     |
| Catechin (Cate)         | 0.5–50                    | 3.46                 | $y = 0.1674x + 0.0143$ | 0.9994                            | 0.06                     | 0.21                     |
| Epicatechin (Epi)       | 0.5–50                    | 3.87                 | $y = 0.0955x + 0.0169$ | 0.9995                            | 0.08                     | 0.25                     |
| Chlorogenic acid (CGA)  | 0.1–50                    | 3.66                 | $y = 0.0778x + 0.0135$ | 0.9995                            | 0.01                     | 0.04                     |
| Caffeic acid (CA)       | 0.5–50                    | 4.76                 | $y = 0.7778x + 0.1366$ | 0.9995                            | 0.09                     | 0.29                     |
| Sinapinic acid (SA)     | 1.0–50                    | 6.10                 | $y = 0.0072x - 0.0021$ | 0.9996                            | 0.29                     | 0.96                     |
| p-Coumaric acid (p-CMA) | 0.5–50                    | 6.46                 | $y = 0.7237x + 0.0232$ | 0.9996                            | 0.18                     | 0.60                     |
| Ferulic acid (FA)       | 0.2–50                    | 6.49                 | $y = 0.1138x + 0.0004$ | 0.9985                            | 0.06                     | 0.20                     |
| Rutin (Ru)              | 0.2–50                    | 7.53                 | $y = 0.1876x + 0.0234$ | 0.9995                            | 0.04                     | 0.14                     |
| Quercetin (Que)         | 0.2–50                    | 9.01                 | $y = 0.1909x - 0.0217$ | 0.9985                            | 0.04                     | 0.14                     |
| Hesperetin (Hes)        | 1.0–50                    | 9.21                 | $y = 0.2423x + 0.0124$ | 0.9987                            | 0.27                     | 0.91                     |

<sup>a</sup> LOD: Limit of detection.

<sup>b</sup> LOQ: Limit of quantification.

Table 2. Phenolic acids and flavonoids in real sample.

|                  | GA<br>(ng/mL) | CGA<br>(ng/mL) | CA<br>(ng/mL) | p-CMA<br>(ng/mL) | FA<br>(ng/mL) | Ru<br>(ng/mL) | Que<br>(ng/mL) | Hes<br>(ng/mL) | SA<br>(ng/mL) | Cate<br>(ng/mL) | Epi<br>(ng/mL) |
|------------------|---------------|----------------|---------------|------------------|---------------|---------------|----------------|----------------|---------------|-----------------|----------------|
| White grape wine | 60.28         | 17.69          | 19.43         | 29.81            | 68.82         | 10.08         | 10.52          | N.D.           | 41.73         | 39.26           | 1.80           |
| Litchi wine      | 41.82         | 4.27           | 7.60          | 14.85            | 74.44         | 0.96          | 4.80           | N.D.           | 19.75         | 2.23            | 1.60           |

N.D.: Not detected.

acids and flavonoids in two fruit wine. Furthermore, after the  $\text{Fe}_3\text{O}_4@\text{pDA}$  step, these interferences were greatly reduced, and the satisfactory results are presented in (Table 2). The phenolic acids and flavonoids concentrations for fruit wine were found to be in the range of 0.91–26.5 ng/L.

#### 4. Conclusions

The results obtained in this work show that magnetic  $\text{Fe}_3\text{O}_4@\text{pDA}$  material was synthesized and applied to a new magnetic adsorbent for the pre-concentration and coupled to LC–MS/MS determination of phenolic acids and flavonoids from two fruit wine samples.

The method provides quite a fast interaction between the phenolic acids, flavonoids and  $\text{Fe}_3\text{O}_4@\text{pDA}$ , and without the need for additional centrifugation. These results demonstrated that the

developed method provides good repeatability and good recovery and can be successfully applied to the determination of phenolic acids and flavonoids in various wine samples.

#### Conflict of interest

The authors declare that they have no conflicts of interest.

#### Acknowledgments

This work was supported by grant MOST 109-2113-M-030-003 and MOST 109-2113-M-030-011 from the Ministry of Science and Technology (MOST), Taiwan. The magnetic measurements were obtained from SQUID (MPMS 3) in NTU.

#### Appendix A. Supplementary material

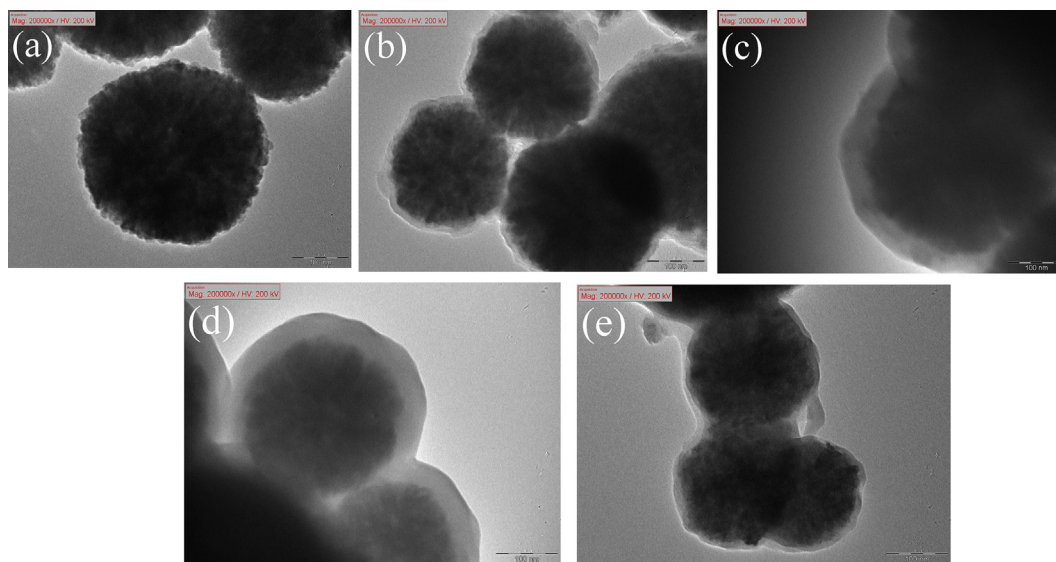


Fig.S1. TEM images of (a)  $\text{Fe}_3\text{O}_4$ , (b)  $\text{Fe}_3\text{O}_4@\text{pDA}$ , (c)  $\text{Fe}_3\text{O}_4@\text{SiO}_2$ , (d)  $\text{Fe}_3\text{O}_4@\text{SiO}_2@\text{C18}$  and (e)  $\text{Fe}_3\text{O}_4@\text{SiO}_2@\text{APTES}$ .



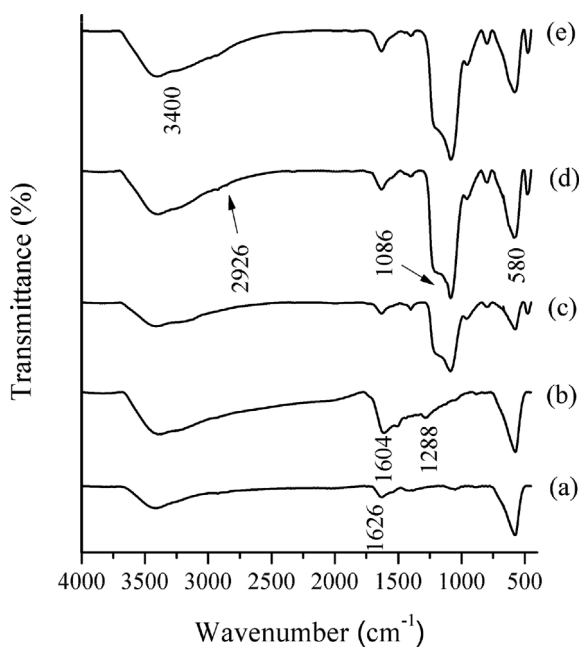


Fig.S2. The FT-IR spectra showed a significant difference (a)  $\text{Fe}_3\text{O}_4$ , (b)  $\text{Fe}_3\text{O}_4@p\text{DA}$ , (c)  $\text{Fe}_3\text{O}_4@SiO_2$ , (d)  $\text{Fe}_3\text{O}_4@SiO_2@C18$  and (e)  $\text{Fe}_3\text{O}_4@SiO_2@APTES$ .

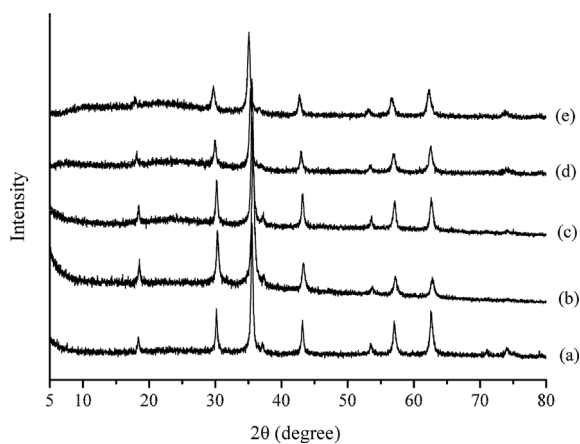


Fig.S3. PXRD characterization was applied to further investigate the composition of (a)  $\text{Fe}_3\text{O}_4$ , (b)  $\text{Fe}_3\text{O}_4@p\text{DA}$ , (c)  $\text{Fe}_3\text{O}_4@SiO_2$ , (d)  $\text{Fe}_3\text{O}_4@SiO_2@C18$  and (e)  $\text{Fe}_3\text{O}_4@SiO_2@APTES$ .

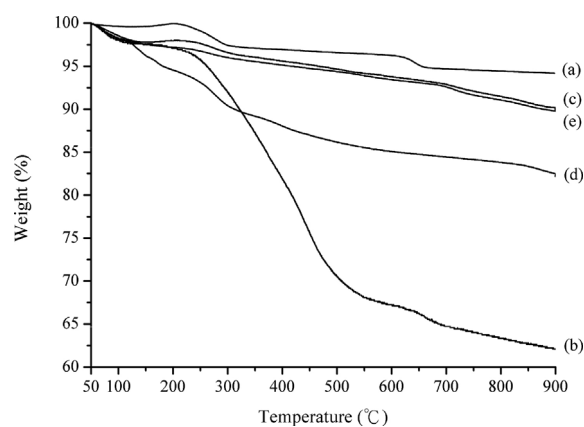


Fig.S4. TGA thermogram of (a)  $\text{Fe}_3\text{O}_4$ , (b)  $\text{Fe}_3\text{O}_4@p\text{DA}$ , (c)  $\text{Fe}_3\text{O}_4@SiO_2$ , (d)  $\text{Fe}_3\text{O}_4@SiO_2@C18$  and (e)  $\text{Fe}_3\text{O}_4@SiO_2@APTES$ .

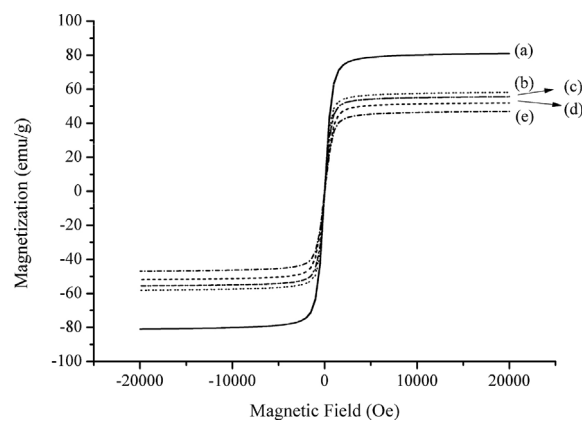


Fig.S5. The magnetic property of (a)  $\text{Fe}_3\text{O}_4$ , (b)  $\text{Fe}_3\text{O}_4@p\text{DA}$ , (c)  $\text{Fe}_3\text{O}_4@SiO_2$ , (d)  $\text{Fe}_3\text{O}_4@SiO_2@C18$  and (e)  $\text{Fe}_3\text{O}_4@SiO_2@APTES$ .

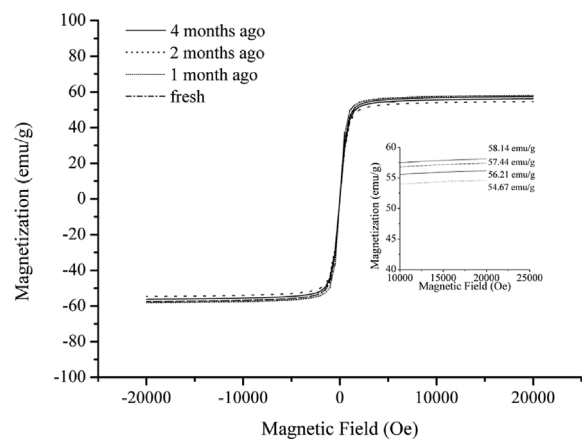


Fig. S6. Influence of reusability on the extraction efficiency.

Table S1. Analytical performance of the method for the phenolic acids and flavonoids in white grape wine.

| Sample           | Analyte | Spike Level (ng/mL) | Intra-day <sup>a</sup> (n = 3) | Inter-day <sup>b</sup> (n = 9) |
|------------------|---------|---------------------|--------------------------------|--------------------------------|
|                  |         |                     | Recovery <sup>c</sup> (%) ± SD | Recovery <sup>c</sup> (%) ± SD |
| White grape wine | GA      | 5                   | 84.07 ± 3.73                   | 86.24 ± 3.61                   |
|                  |         | 20                  | 114.86 ± 3.50                  | 115.06 ± 0.96                  |
|                  |         | 100                 | 115.43 ± 2.67                  | 115.46 ± 2.33                  |
|                  | CGA     | 5                   | 87.50 ± 2.87                   | 84.78 ± 8.55                   |
|                  |         | 20                  | 110.84 ± 1.83                  | 109.52 ± 6.67                  |
|                  |         | 100                 | 113.70 ± 2.85                  | 112.02 ± 8.86                  |
|                  | CA      | 5                   | 84.42 ± 3.26                   | 80.33 ± 4.90                   |
|                  |         | 20                  | 109.22 ± 1.73                  | 107.54 ± 2.98                  |
|                  |         | 100                 | 110.54 ± 1.12                  | 110.30 ± 4.35                  |
|                  | p-CMA   | 5                   | 107.56 ± 4.85                  | 116.73 ± 9.44                  |
|                  |         | 20                  | 114.01 ± 1.82                  | 119.69 ± 4.96                  |
|                  |         | 100                 | 115.65 ± 0.51                  | 120.78 ± 6.42                  |
|                  | FA      | 5                   | 95.86 ± 6.47                   | 80.62 ± 6.71                   |
|                  |         | 20                  | 112.53 ± 5.66                  | 114.78 ± 2.67                  |
|                  |         | 100                 | 116.68 ± 4.87                  | 112.48 ± 6.74                  |
|                  | Ru      | 5                   | 93.39 ± 2.38                   | 99.06 ± 6.82                   |
|                  |         | 20                  | 108.78 ± 7.17                  | 115.18 ± 7.35                  |
|                  |         | 100                 | 107.24 ± 3.52                  | 115.58 ± 8.44                  |
|                  | Que     | 5                   | 88.95 ± 3.00                   | 89.10 ± 0.03                   |
|                  |         | 20                  | 88.21 ± 6.00                   | 97.38 ± 9.45                   |
|                  |         | 100                 | 104.99 ± 4.86                  | 114.08 ± 9.86                  |
|                  | Hes     | 5                   | 88.92 ± 4.53                   | 88.46 ± 4.19                   |
|                  |         | 20                  | 114.31 ± 4.32                  | 115.67 ± 4.41                  |
|                  |         | 100                 | 113.04 ± 3.18                  | 111.66 ± 6.03                  |
|                  | SA      | 5                   | 85.24 ± 14.08                  | 82.17 ± 4.46                   |
|                  |         | 20                  | 83.42 ± 2.39                   | 75.09 ± 7.65                   |
|                  |         | 100                 | 108.88 ± 6.21                  | 112.04 ± 9.05                  |
| Cate             | 5       | 113.91 ± 1.27       | 94.30 ± 7.34                   |                                |
|                  | 20      | 113.21 ± 3.15       | 99.15 ± 1.57                   |                                |
|                  | 100     | 84.94 ± 1.51        | 86.24 ± 7.20                   |                                |
| Epi              | 5       | 105.30 ± 6.91       | 101.64 ± 13.21                 |                                |
|                  | 20      | 82.27 ± 5.39        | 88.04 ± 7.36                   |                                |
|                  | 100     | 80.03 ± 3.38        | 84.94 ± 7.20                   |                                |

<sup>a</sup> n = 3 extractions in the same day.<sup>b</sup> n = 9 extractions in 3 consecutive days.<sup>c</sup> Recovery (%) = (spike sample conc. – non-spike sample conc.)/spike conc. × 100%.

Table S2. Analytical performance of the method for the phenolic acids and flavonoids in litchi wine.

| Sample      | Analyte | Spike Level (ng/mL) | Intra-day <sup>a</sup> (n = 3) | Inter-day <sup>b</sup> (n = 9) |
|-------------|---------|---------------------|--------------------------------|--------------------------------|
|             |         |                     | Recovery <sup>c</sup> (%) ± SD | Recovery <sup>c</sup> (%) ± SD |
| Litchi wine | GA      | 5                   | 105.45 ± 6.76                  | 107.03 ± 5.33                  |
|             |         | 20                  | 95.98 ± 4.48                   | 91.02 ± 9.46                   |
|             |         | 100                 | 89.87 ± 7.36                   | 89.25 ± 2.37                   |
|             | CGA     | 5                   | 102.91 ± 1.67                  | 119.42 ± 5.96                  |
|             |         | 20                  | 93.65 ± 1.22                   | 113.81 ± 7.49                  |
|             |         | 100                 | 94.54 ± 4.65                   | 110.81 ± 4.09                  |
|             | CA      | 5                   | 111.86 ± 2.44                  | 112.88 ± 2.73                  |
|             |         | 20                  | 102.73 ± 0.48                  | 107.07 ± 3.96                  |
|             |         | 100                 | 104.99 ± 2.88                  | 105.32 ± 0.52                  |
|             | p-CMA   | 5                   | 102.71 ± 8.39                  | 111.68 ± 8.22                  |
|             |         | 20                  | 105.56 ± 1.19                  | 111.98 ± 5.70                  |
|             |         | 100                 | 107.04 ± 4.42                  | 110.84 ± 7.14                  |
|             | FA      | 5                   | 104.66 ± 8.17                  | 108.13 ± 6.19                  |
|             |         | 20                  | 108.06 ± 6.43                  | 102.82 ± 5.79                  |
|             |         | 100                 | 111.26 ± 3.99                  | 108.28 ± 3.93                  |
|             | Ru      | 5                   | 116.10 ± 7.25                  | 114.72 ± 3.22                  |
|             |         | 20                  | 95.59 ± 0.68                   | 101.54 ± 5.17                  |
|             |         | 100                 | 101.28 ± 2.10                  | 103.02 ± 1.52                  |

(continued on next page)

Table S2. (continued)

| Sample | Analyte | Spike Level (ng/mL) | Intra-day <sup>a</sup> (n = 3) | Inter-day <sup>b</sup> (n = 9) |
|--------|---------|---------------------|--------------------------------|--------------------------------|
|        |         |                     | Recovery <sup>c</sup> (%) ± SD | Recovery <sup>c</sup> (%) ± SD |
|        | Que     | 5                   | 105.45 ± 9.68                  | 107.03 ± 6.41                  |
|        |         | 20                  | 95.98 ± 4.68                   | 91.02 ± 8.61                   |
|        |         | 100                 | 89.87 ± 7.52                   | 89.25 ± 2.12                   |
|        | Hes     | 5                   | 100.28 ± 9.11                  | 111.30 ± 9.57                  |
|        |         | 20                  | 102.92 ± 8.97                  | 108.95 ± 5.68                  |
|        |         | 100                 | 98.89 ± 8.83                   | 102.37 ± 3.17                  |
|        | SA      | 5                   | 84.00 ± 9.93                   | 103.04 ± 6.51                  |
|        |         | 20                  | 87.90 ± 5.97                   | 83.55 ± 3.93                   |
|        |         | 100                 | 113.63 ± 7.25                  | 112.65 ± 8.45                  |
|        | Cate    | 5                   | 98.99 ± 6.60                   | 114.86 ± 8.19                  |
|        |         | 20                  | 99.89 ± 8.74                   | 100.88 ± 8.54                  |
|        |         | 100                 | 92.56 ± 8.31                   | 97.41 ± 4.23                   |
|        | Epi     | 5                   | 103.11 ± 9.36                  | 98.84 ± 8.36                   |
|        |         | 20                  | 106.11 ± 9.84                  | 112.58 ± 9.25                  |
|        |         | 100                 | 102.01 ± 3.29                  | 101.87 ± 5.42                  |

<sup>a</sup> n = 3 extractions in the same day.

<sup>b</sup> n = 9 extractions in 3 consecutive days.

<sup>c</sup> Recovery (%) = (spike sample conc. – non-spike sample conc.)/spike conc. × 100%.

## References

- [1] Shahidi F, Yeo J. Bioactivities of phenolics by focusing on suppression of chronic diseases: a review. *Int J Mol Sci* 2018; 19.
- [2] Rai S, Kureel AK, Dutta PK, Mehrotra GK. Phenolic compounds based conjugates from dextran aldehyde and BSA: preparation, characterization and evaluation of their anticancer efficacy for therapeutic applications. *Int J Biol Macromol* 2018;110:425–36.
- [3] Skoog Dah FJ, Crouch SR. Principle of instrumental analysis. 6 ed. David Harris; 2007.
- [4] Eroğlu C, Seçme M, Bağcı G, Dodurga Y. Assessment of the anticancer mechanism of ferulic acid via cell cycle and apoptotic pathways in human prostate cancer cell lines. *Tumor Biol* 2015;36:9437–46.
- [5] Pedan V, Popp M, Rohn S, Nyfeler M, Bongartz A. Characterization of phenolic compounds and their contribution to sensory properties of olive oil. *Molecules* 2019;24.
- [6] Soto-Vaca A, Gutierrez A, Losso JN, Xu Z, Finley JW. Evolution of phenolic compounds from color and flavor problems to health benefits. *J Agric Food Chem* 2012;60:6658–77.
- [7] Khezeli T, Daneshfar A, Sahraei R. A green ultrasonic-assisted liquid–liquid microextraction based on deep eutectic solvent for the HPLC-UV determination of ferulic, caffeic and cinnamic acid from olive, almond, sesame and cinnamon oil. *Talanta* 2016;150:577–85.
- [8] Sas OG, Domínguez I, González B, Domínguez Á. Liquid-liquid extraction of phenolic compounds from water using ionic liquids: literature review and new experimental data using [C2mim]FSI. *J Environ Manag* 2018;228:475–82.
- [9] Soltani R, Shahvar A, Dinari M, Saraji M. Environmentally-friendly and ultrasonic-assisted preparation of two-dimensional ultrathin Ni/Co-NO<sub>3</sub> layered double hydroxide nanosheet for micro solid-phase extraction of phenolic acids from fruit juices. *Ultrason Sonochem* 2018;40:395–401.
- [10] Dai X, Wang D, Li H, Chen Y, Gong Z, Xiang H, et al. Hollow porous ionic liquids composite polymers based solid phase extraction coupled online with high performance liquid chromatography for selective analysis of hydrophilic hydroxybenzoic acids from complex samples. *J Chromatogr A* 2017;1484:7–13.
- [11] Dahmoune F, Nayak B, Moussi K, Remini H, Madani K. Optimization of microwave-assisted extraction of polyphenols from *Myrtus communis* L. leaves. *Food Chem* 2015; 166:585–95.
- [12] Ranjbar Banforuzi S, Hadjmohammadi MR. Two-phase hollow fiber-liquid microextraction based on reverse micelle for the determination of quercetin in human plasma and vegetables samples. *Talanta* 2017;173:14–21.
- [13] Li M m, Hu S, Chen X, Bai X h. Development of a novel hollow-fiber liquid-phase microextraction based on oil-in-salt and its comparison with conventional one. *J Separ Sci* 2017;40:2941–9.
- [14] Li J, Jia S, Yoon SJ, Lee SJ, Kwon SW, Lee J. Ion-pair dispersive liquid–liquid microextraction solidification of floating organic droplets method for the rapid and sensitive detection of phenolic acids in wine samples using liquid chromatography combined with a core–shell particle column. *J Food Compos Anal* 2016;45:73–9.
- [15] Silva B, Gonzaga LV, Fett R, Oliveira Costa AC. Improved strategy based on QuEChERS method followed by HPLC/DAD for the quantification of phenolic compounds from *Mimosa scabrella* Benth honeydew honeys. *LWT* 2019;116:108471.
- [16] Song JG, Cao C, Li J, Xu YJ, Liu Y. Development and validation of a QuEChERS-LC-MS/MS method for the analysis of phenolic compounds in rapeseed oil. *J Agric Food Chem* 2019;67:4105–12.
- [17] Kuo YC, Heish WQ, Huang HY, Liu WL. Application of mesoporous carbon-polymer monolith for the extraction of phenolic acid in food samples. *J Chromatogr A* 2018;1539: 12–8.
- [18] Hosny H, El Gohary N, Saad E, Handoussa H, El Nashar RM. Isolation of sinapic acid from broccoli using molecularly imprinted polymers. *J Separ Sci* 2018;41:1164–72.
- [19] Hou X, Wang X, Sun Y, Wang L, Guo Y. Graphene oxide for solid-phase extraction of bioactive phenolic acids. *Anal Bioanal Chem* 2017;409:3541–9.
- [20] Hernández-Hernández AA, Álvarez-Romero GA, Contreras-López E, Aguilar-Arteaga K, Castañeda-Ovando A. Food analysis by microextraction methods based on the use of magnetic nanoparticles as supports: recent advances. *Food Anal Methods* 2017;10:2974–93.
- [21] Li W, Zhang J, Zhu W, Qin P, Zhou Q, Lu M, et al. Facile preparation of reduced graphene oxide/ZnFe<sub>2</sub>O<sub>4</sub> nanocomposite as magnetic sorbents for enrichment of estrogens. *Talanta* 2020;208:120440.
- [22] Chai W, Wang H, Zhang Y, Ding G. Preparation of polydopamine-coated magnetic nanoparticles for dispersive solid-phase extraction of water-soluble synthetic colorants in beverage samples with HPLC analysis. *Talanta* 2016;149: 13–20.

- [23] González-Sálamo J, Socas-Rodríguez B, Hernández-Borges J, Rodríguez-Delgado MÁ. Core-shell poly(dopamine) magnetic nanoparticles for the extraction of estrogenic mycotoxins from milk and yogurt prior to LC–MS analysis. *Food Chem* 2017;215:362–8.
- [24] Yavuz E, Tokaloğlu Ş, Patat Ş. Core-shell Fe<sub>3</sub>O<sub>4</sub> polydopamine nanoparticles as sorbent for magnetic dispersive solid-phase extraction of copper from food samples. *Food Chem* 2018;263:232–9.
- [25] Zhang S, Yao W, Ying J, Zhao H. Polydopamine-reinforced magnetization of zeolitic imidazolate framework ZIF-7 for magnetic solid-phase extraction of polycyclic aromatic hydrocarbons from the air-water environment. *J Chromatogr A* 2016;1452:18–26.
- [26] Wang Q, Zhang R, Lu M, You G, Wang Y, Chen G, et al. Bioinspired polydopamine-coated hemoglobin as potential oxygen carrier with antioxidant properties. *Biomacromolecules* 2017;18:1333–41.
- [27] Huang Z, Lee HK. Study and comparison of polydopamine and its derived carbon decorated nanoparticles in the magnetic solid-phase extraction of estrogens. *J Chromatogr A* 2015;1414:41–50.
- [28] Kumar DR, Kesavan S, Nguyen TT, Hwang J, Lamiel C, Shim JJ. Polydopamine@electrochemically reduced graphene oxide-modified electrode for electrochemical detection of free-chlorine. *Sensor Actuator B Chem* 2017;240:818–28.
- [29] Wu M, Zhang D, Zeng Y, Wu L, Liu X, Liu J. Nanocluster of superparamagnetic iron oxide nanoparticles coated with poly (dopamine) for magnetic field-targeting, highly sensitive MRI and photothermal cancer therapy. *Nanotechnology* 2015;26:115102.
- [30] Subair R, Tripathi BP, Formanek P, Simon F, Uhlmann P, Stamm M. Polydopamine modified membranes with in situ synthesized gold nanoparticles for catalytic and environmental applications. *Chem Eng J* 2016;295:358–69.
- [31] Socas-Rodríguez B, Hernández-Borges J, Herrera-Herrera AV, Rodríguez-Delgado MÁ. Multiresidue analysis of oestrogenic compounds in cow, goat, sheep and human milk using core-shell polydopamine coated magnetic nanoparticles as extraction sorbent in micro-dispersive solid-phase extraction followed by ultra-high-performance liquid chromatography tandem mass spectrometry. *Anal Bioanal Chem* 2018;410:2031–42.
- [32] Wang Y, Wang S, Niu H, Ma Y, Zeng T, Cai Y, et al. Preparation of polydopamine coated Fe<sub>3</sub>O<sub>4</sub> nanoparticles and their application for enrichment of polycyclic aromatic hydrocarbons from environmental water samples. *J Chromatogr A* 2013;1283:20–6.
- [33] Rasouli H, Farzaei MH, Khodarahmi R. Polyphenols and their benefits: a review. *Int J Food Prop* 2017;20:1700–41.
- [34] Aslani E, Abri A, Pazhang M. Immobilization of trypsin onto Fe<sub>3</sub>O<sub>4</sub>@SiO<sub>2</sub> –NH<sub>2</sub> and study of its activity and stability. *Colloids Surf B Biointerfaces* 2018;170:553–62.
- [35] Guo B, Ji S, Zhang F, Yang B, Gu J, Liang X. Preparation of C18-functionalized Fe<sub>3</sub>O<sub>4</sub>@SiO<sub>2</sub> core-shell magnetic nanoparticles for extraction and determination of phthalic acid esters in Chinese herb preparations. *J Pharmaceut Biomed Anal* 2014;100:365–8.
- [36] Guidance for industry : bioanalytical method validation. Center for drug E, research, center for veterinary M. Rockville, MD: U.S. Dept. of Health and Human Services, Food and Drug Administration, Center for Drug Evaluation and Research : Center for Veterinary Medicine; 2001.
- [37] Roselló-Soto E, Martí-Quijal JF, Cilla A, Munekata ESP, Lorenzo MJ, Remize F, et al. Influence of temperature, solvent and pH on the selective extraction of phenolic compounds from tiger nuts by-products: triple-TOF-LC-MS-MS characterization. *Molecules* 2019;24.